

Characterization Studies of Integrated Hydroxyapatite FROM Fish Scale and Polyether Sulfone Membrane for Ion Exchange Membrane Preparation

Open
Access

Sofiah Hamzah^{1,*}, Mohd Sabri Mohd Ghazali^{2,3}, Norhafiza Ilyana Yatim³, Jamali Sukaimi¹, Maslinda Alias¹

¹ School of Ocean Engineering, Universiti Malaysia Terengganu, 21030 Kuala Nerus, Terengganu, Malaysia

² School of Fundamental Science, Universiti Malaysia Terengganu, 21030 Kuala Nerus, Terengganu, Malaysia

³ Institute of Tropical Biodiversity and Sustainable Development, Universiti Malaysia Terengganu, 21030 Kuala Nerus, Terengganu, Malaysia

⁴ School of Environmental and Marine Science, Universiti Malaysia Terengganu, 21030 Kuala Nerus, Terengganu, Malaysia

ARTICLE INFO

ABSTRACT

Article history:

Received 5 June 2019

Received in revised form 4 July 2019

Accepted 12 July 2019

Available online 3 December 2019

Keywords:

Membrane; hydroxyapatite; PES; ion exchange; protease

This study aimed to integrate polyether sulfone (PES) membrane with hydroxyapatite synthesized from fish scale biowaste (HAp) to form ion exchange membrane. The PES incorporated by self-assembled with different concentrations of HAp solution; 0.2, 0.4, 0.6, 0.8 and 1.0 wt%. The prepared ion exchange membranes were characterized regarding permeability coefficient, porosity, morphology, ion exchange capacity (IEC), AT-IR, and fouling analysis. The promising characteristics and outstanding performance demonstrated by PES membrane incorporated with 0.8 wt%. Via SEM images and AT-IR spectra, the PES/HAp-0.8 membrane depicted the adequate number, well distributed and low agglomeration of HAp onto the membrane surface with a strong attachment. The membrane also demonstrated good ion exchange capacity around 49%. Permeability coefficient for PES/HAp-0.8 membrane was 101.5 L/m².h with 87.69 % membrane porosity.

Copyright © 2019 PENERBIT AKADEMIA BARU - All rights reserved

1. Introduction

Downstream processing is one of the most challenging parts in enzyme and protein production [1] due to the complicated process, long processing time, and often required high installment of equipment. Therefore, many researchers seek out a novel and fine method as to solve these issues and recently, the focus is on the chromatographic membrane [2]. Basically, this unique and fine technology work by allowing the interested molecule pass through the membrane and trapped impurities that present in the enzyme solution [3]. The effectiveness of the process is highly depends on the adsorptive material used and the structural properties of the membrane itself.

One of the most important considerations in developing this finest available technology is the selection of matrix material for affinity membrane in which larger pores and low fouling

* Corresponding author.

E-mail address: sofiah@umt.edu.my (Sofiah Hamzah)

characteristics of the membrane are required. Recently, many industry application demands to utilize matrix that is made up from synthetic polymers such as poly (vinylidene fluoride) (PVDF), polysulfone (PSU), poly(ethersulfone) (PES) or polysaccharide such as cellulose acetate which able to promote a good separation performance. These polymeric membranes can offer great chemical resistance, high thermal toleration, less susceptible to biological attack, high recovery and great mechanical strength [4-6]. For the fabrication of ion exchange membrane, the most crucial part is deciding the functional groups that will be used as charged exchanger since the ion exchange process will be determined by the nature of the existing functional group [7]. The adsorbent material must be highly selective so that it can only bind to target enzyme as to achieve high degree protein purification [8]. The aim of this technique is not only to specifically bind the target enzyme from its mixture but also to release and unbound the isolated target in an active form [9].

Recently, researchers have discovered a new and high potential material which is HAp to be used as an adsorbent for IExM [10]. HAp has good adsorption to protein because of its biocompatibility, bioactivity, and osteoconductivity [10]. Due to their availability structure, ionic exchange property, adsorption affinity, and their characteristic to establish bonds with organic molecules of different sizes have conferred to this material to have high potential to be used as an adsorbent material for IExM [11]. Natural HAp has recently been extracted from fish scale [12] due to the fact that these biowaste products contain calcite salt and biologically safe since there is no chemicals are required and a potentially lucrative process [13].

In this study, the membrane was fabricated by using PES polymeric material with 15 wt% concentration and casted into a flat sheet by using dry/wet phase technique. Meanwhile, Hap extracted from fish scale biowaste was prepared by using alkaline heat method with 300 °C calcination temperature. HAp solution was prepared at five different concentrations and the membrane was modified by self-assembled technique. The prepared membranes were characterized in term of permeability coefficient, fouling quantification, membrane porosity, morphology, ion exchange capacity, the presence of functional group and crystallinity test.

2. Methodology

2.1 Material

Fish scale waste was freshly collected from a local market in Kuala Terengganu province located at Northeastern Malaysia. The membrane was fabricated by using high-purity grade polymeric material PES and N-methyl-2-Pyrrolidone (NMP) as a solvent. Acetic acid, Hydrochloric acid, and sodium hydroxide were used for modification stage. Commercial protease from bacillus was used for membrane performance evaluation.

2.2 Preparation of HAp/PES Ion Exchange Membrane

The fish scale was freshly collected from the market in Kuala Terengganu. Hap was extracted from fish scale by alkaline heat treatment method followed by a sintering process at 300°C for 1 hour, as described in the previous study [12]. Fabrication of PES15 membrane and its integration with the extracted HAp followed the procedure of the previous study [14]. The HAp solutions were prepared by dissolving HAp in five different concentrations (0.2, 0.4, 0.6, 0.8 and 1.0 mg/mL) in acetic acid at pH 5. The HAp particles were deposited on the membrane surface and then the hybrid membrane was dried at room temperature overnight. Next, the dried membrane was neutralized with NaOH solution followed by rinsing with 50% (v/v) ethanol solution for 3 times. This step also helps to

remove any NaOH that remained on the IExM. The IExM was stored in the distilled water for characterization and performance tests.

2.3 Characterization of HAp/PES IExM

2.3.1 Pure water flux and membrane porosity measurement

The flux of IExM was measured by using dead-end filtration cell with an effective membrane area of 14.6 cm² and the cell was positioned in a U-shaped configuration. Distilled water was used for pure water permeation test to obtain pure water permeability and to ensure membrane stability. Distilled water was drawn through the membrane with compressed nitrogen, controlled in the range 1 to 5 bar. The pure water flux was calculated by using equation 1:

$$J_w = P_m \Delta P \quad (1)$$

Where, pure water flux J_w is expressed in unit m³/m²s, P_m is the permeability (m³/m²s .bar) and ΔP is the pressure (bars). The porosity of pristine and modified membrane was evaluated by their capacity for water absorption and calculated using the expression: [15]

$$\text{Porosity} = [(W_1 - W_2) / d_{\text{water}}] / v \times 100 \quad (2)$$

where W_1 and W_2 are the mass of membrane in the wet and dry states, respectively, d_{water} is the density of water at 20 °C and V is the volume of the membrane in the wet state.

2.3.2 Membrane morphology inspection

Scanning electron microscopy (SEM) (JSM P/N HP475 model) in Institute of Oceanography, Universiti Malaysia Terengganu (UMT) was used to inspect the cross-section image of the in-house fabricated membrane. For this purpose, the membrane samples were fractured in liquid nitrogen with estimated dimension 2mm x 2mm and sputtered with gold, before transferred to the microscope.

2.3.3 ATR-FTIR and XRD analysis

The elemental content of modified membranes was also characterized using a wide angle X-ray diffractometer (XRD) using 18 kW CuK α radiation as described by Hamzah *et al.*, [17]. The voltage was 45 kV and the intensity 40 mA. The angle of diffraction (2θ) varied from 0 to 80° to identify any changes in crystal morphology and intermolecular distances between inter-segmental chains of the polymer, and the counting time was 1 s at each angle step. For comparison purposes, XRD was performed on HAp particles, pristine PES membrane, and PES/ HAp hybrid membrane. The functional groups on the membrane surface were determined using Fourier transform infrared spectroscopy equipped with attenuated total reflection (ATR-FTIR).

2.3.4 Determination of ion exchange capacity

After rinsing in pure water for one day, a membrane sample was soaked in a large volume of 1 N HCl solution for 1 day to obtain a membrane in the H⁺ form. The excess HCl in the membrane was removed by repeated washing with pure water. The membrane in the H⁺-form was then immersed

in 1 N NaOH solution at room temperature for 15, 30, 45, 60 and 75 hours. The membrane was then taken out, and the NaOH solution was titrated with 0.1 N HCl solution with a drop of phenolphthalein solution (0.1% in ethanol) as a pH indicator. The sample was dried at 50°C under vacuum and weighed. The IEC (*meq/g*) was calculated according to the following equation [15]:

$$IEC = [(V_{NaOH} \times N_{NaOH}) - (V_{HCl} \times N_{HCl})] / \text{weight of sample} \quad (3)$$

Where N_{NaOH} and N_{HCl} are the concentrations of the NaOH and HCl solutions, respectively, and V_{HCl} and V_{NaOH} are the volumes of HCl and NaOH solutions, respectively.

2.4 Fouling Quantification

Fouling is the most critical problem during membrane separation process and this resistance appeared by the formation of cake layer or gel layer on the membrane surface. For fouling quantification, procedures described by Hamzah *et al.*, [16] have been followed. Pure water permeation was conducted at a constant pressure of 5 bar. Pure water flux was obtained from the volume of permeated water within 30 min and calculated as

$$J_0 = Q / (At) \quad (4)$$

where J_0 is pure water flux, Q is the permeate volume, A is membrane area and t is the time. After water flux measurement (J_0), the solution reservoir was refilled with 0.5 mg mL⁻¹ protease solution. After 30 min filtration, the membrane was cleaned by shaking in pure water for 2 h at 25 °C and then pure water fluxes (J_1) were measured again. By comparing the value of J_0 and J_1 , flux recovery ratio can be determined by using equation (2)

$$FRR (\%) = (J_0 / J_1) \times 100 \quad (5)$$

$$RFR (\%) = [1 - (J_0 / J_1)] \times 100 \quad (6)$$

3. Results and Discussion

3.1 Membrane Morphology and Structure

Figure 1 shows the surface morphology of native PES and modified PES with different concentrations of hydroxyapatite extracted from fish scales.

The least amount of the deposited HAp particles can be observed on both PES/HAp-0.2 and 0.4 IExMs. These membranes were less favored since it only occupied a small number of HAp particles which in turn would reduce the separation performance of membranes. According to Nagahama *et al.*, [17], HAp has hydroxyl group which has high tendency and affinity to form hydrogen bonds with water, consequently, helps to improve the structure and morphology of the IExM. It also promoted the cake formation and membrane fouling as a longer time is required for the separation process. PES/HAp-0.6 IExM shows a moderate amount of deposited HAp. However, Figure 2(d) displayed high agglomeration rate of HAp particles. It was postulated that HAp agglomeration which looks like a snowflakes will increase the size particles which in turn will reduce the surface area of adsorption site, therefore diminish the separation rate. The SEM image in Figure 2(e), PES/HAp0.8 shows well uniform distribution and low agglomeration rate. According to Luo *et al.*, [18], the membrane that has these morphologies was believed to be suitable membrane for separation with low membrane fouling.

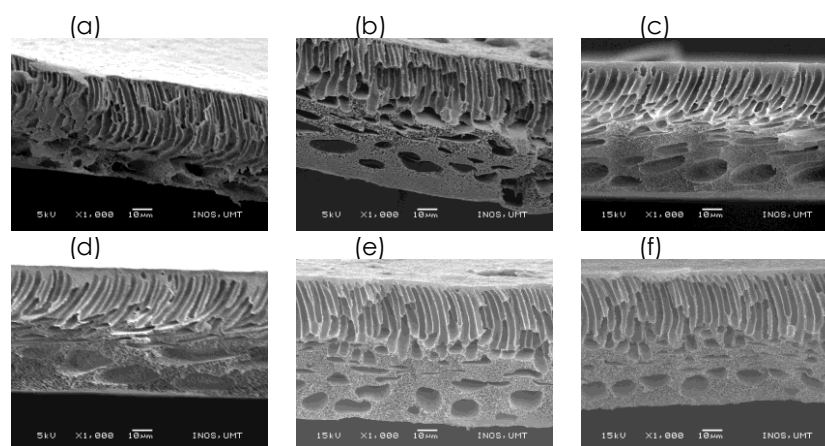


Fig.1. Cross Section Morphologies of (a) PES 15, (b) PES/HAp-0.2, (c) PES/HAp-0.4, (d) PES/HAp-0.6, (e) PES/HAp-0.8, (f) PES/HAp-1.0

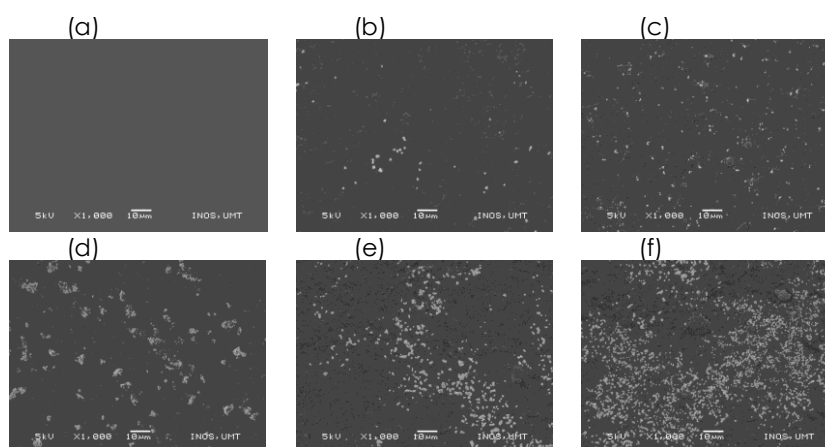


Fig. 2 Surface Morphologies of (a) PES 15, (b) PES/HAp-0.2, (c) PES/HAp-0.4, (d) PES/HAp-0.6, (e) PES/HAp-0.8, (f) PES/HAp-1.0

On the surface of PES/HAp-1.0 IExM, high amount of deposited HAp particles on IExM surface led to poor performance of the membrane. This finding was in agreement with the permeability result by pure water flux measurement. According to Swain and Sankar *et al.*, [19], high amount of HAp blocked the pores of IExM, consequently, this will promote the membrane to foul. It also made the duration for permeation to occur in much longer time.

3.2 AT-IR and XRD Analyses

The FTIR-ATR technique is widely used to study changes that take place on polymer surfaces during modification processes. The new bands that detected after membrane modification indicate the presence of thin layer successfully incorporated on top of the PES membrane. There are three peaks or bands used to determine the characteristics of IExMs; bands for HAp, PES and new peaks that indicated incorporation of HAp onto the PES membrane. The spectra of HAp can be revealed based on the various vibrational modes of hydroxyl groups and phosphates. Bands characteristics to the phosphate and hydrogen phosphate groups in the apatitic environment were observed either at 557 cm^{-1} , 629 cm^{-1} , 605 cm^{-1} or 960 cm^{-1} and bands ranging from 1000–1100 cm^{-1} specifically associated with the PO_4^{3-} groups. The peak around 875 cm^{-1} indicated the presence of HPO_4 group. The presence of strong OH^- vibration at 3200–3600 cm^{-1} can be observed for all IExMs. The broad

bands in the regions 1600–1700 cm^{-1} and correspond to H–O–H bands of water lattice. Asymmetric and symmetric stretching vibration of CH_3 gave their peaks just below 3000 cm^{-1} while the band observed between 2942 and 2944 cm^{-1} corresponds to C–H stretching band. A new peak of stretching band was observed at 2944 cm^{-1} when the FHAp was incorporated. This corresponds to the chemical bond arise from the interactions between HAp particles and PES membrane. The peaks appeared at 2891, 2737, 2692, 1343 cm^{-1} are attributed to different vibration modes of C–H bond of PES. The peaks at 1283 and 1241 cm^{-1} belong to C–C bond.

3.3 XRD Analysis

XRD analysis was used to determine the level of crystallinity of HAp that had been successfully deposited onto the IExM. The XRD patterns of hybrid IExM with the different concentration of FHSAp were shown in Figure 4. Based on these five diffraction patterns, there is reflection corresponding to HAp which indicates that HAp was present on the PES membrane surface. Furthermore, the degree of the crystallinity of HAp can be directly observed via the XRD spectra. Diffraction peaks in the planes 002, 211, 112 and 300 are high and narrow implying that the HAp crystallizes well.

All the patterns displayed the presence of amorphous phases with several diffraction peaks that associating the PES membrane. Figure 4a represented XRD spectra for PES/HAp-0.2 IExM, which is the lowest HAp solution used to modify the PES membrane. From the spectra, it showed low intensity and short peaks at 22.34° and 37.5°. These intense broad reflection peaks which were just below 20° were assigned to PES material. It showed the intensity decreased as the HAp content increased. The XRD spectrum of PES/HAp-0.4 IExM was displayed in the Figure 4b. This spectrum showed some improvement regarding crystallinity of HAp deposited on the PES membrane when compared with PES/HAp-0.2 IExM.

The peaks corresponding to HAp particles were observed at 23.4, 31.9, and 36.3°. The peak intensity and full width at half maxima (FWHM) increased as the concentration of HAp solution used increased. This pattern of the peak intensity and FWHM was due to the increasing behavior of crystallite size of HAp. The amorphous characteristic of the polymer matrix showed decrease trend as the amount of HAp particles increased. Apparently, it was attributed to the interaction between the filler and the polymer through weak van der Waals interaction [20].

Figure 4c shows the XRD patterns of the PES/HAp-0.6 IExM. The spectra showed a broad diffraction peaks at 23.4, 31.8 and 35.8° which is assigned to the crystallographic plane of HAp crystallites. This IExM showed some improvement regarding the intensity and sharpness of the diffraction peaks of FHSAp which indicating the concentration of 0.6 wt% promotes excellence characteristics for PES membrane. However, the modification does alter the crystal structure of the HAp when compared with XRD spectra produced by the HAp. For the Figure 4e, the pattern showed three relative sharp peaks appear at 33.8, 34.7 and 35.1° which are assigned to the (002) and (112) crystalline planes of HAp crystals respectively. It showed that the crystallinity of the HAp only decreases slightly Based on the half width of the (112) reflection peak, the average crystallite size of the HAp crystals on the SFHAp/PES IExM is 23.7 nm, as calculated by the Sherrer equation. XRD spectra of PES/HAp-1.0 IExM showed a quite promising result. The amorphous phase in the spectra corresponds to the polymeric material, PES. There are several sharp peaks with high intensities of isolated diffraction peaks observed in this spectrum. These peaks detected at 21.4, 35.3, 36.1 and 37.4° which are associated with the HAp crystals [21]. However, when compared with the pattern of pure HAp, these peaks were weaker since HAp particles exhibited highly agglomeration rate which diminished the Hap crystallinity. Thus, short and weaker peaks formed.

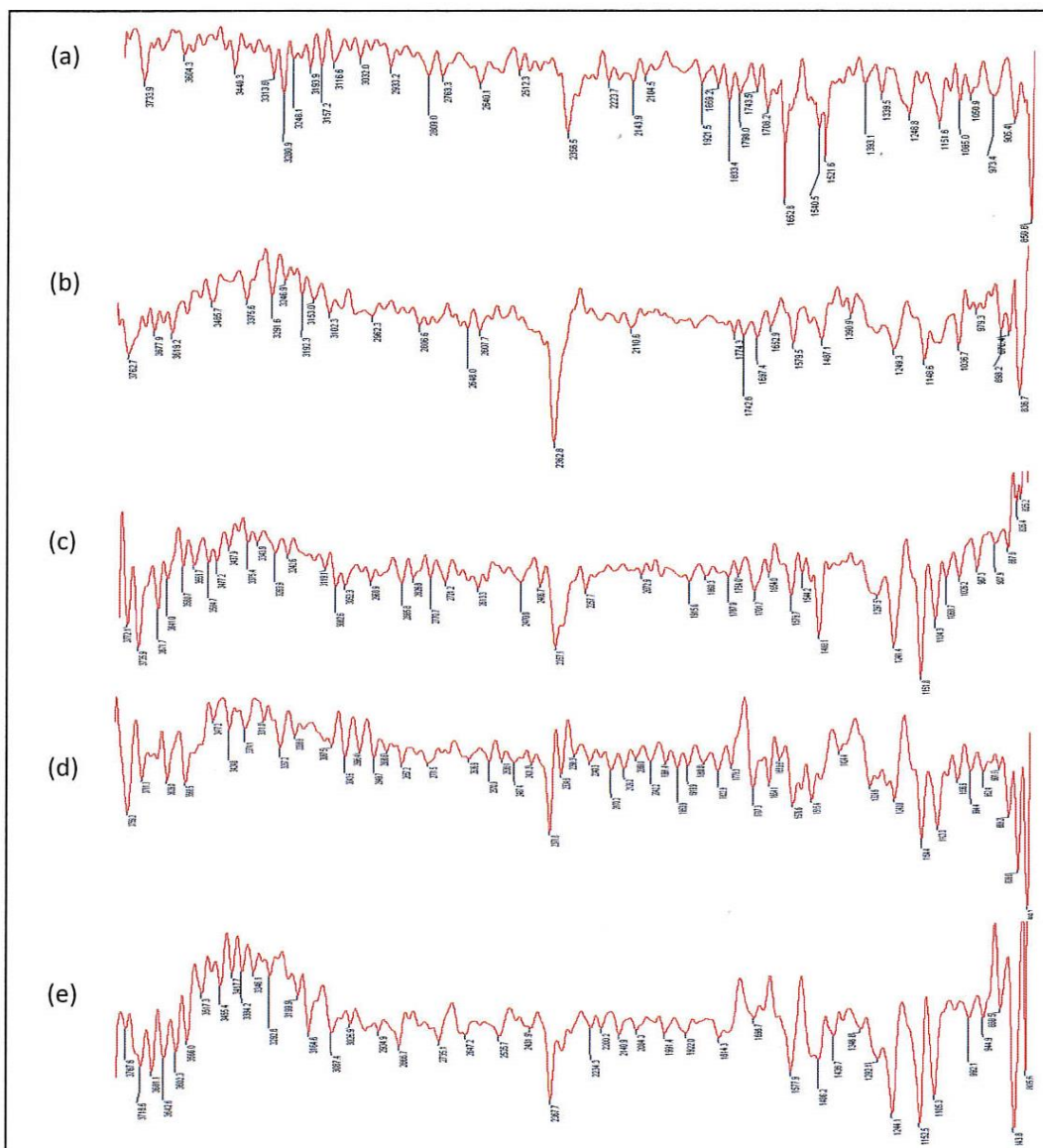


Fig.3. AT-IR spectra for FHSap/PES (a) 0.2, (b) 0.4, (c) 0.6, (d) 0.8 and (e) 1.0 IEXMs

The spectra for PES/HAp-0.8 displayed a sharp and narrow diffraction peaks which indicate the excellent crystallinity for the HAp and well-ordered particles. All peaks allocate at standard diffraction angles for HAp were at 21.7, 35.4, 36.6 and 37.9°. This indicates that the concentration of HAp enhances the obtained particle crystallinity as deposited on the PES membrane.

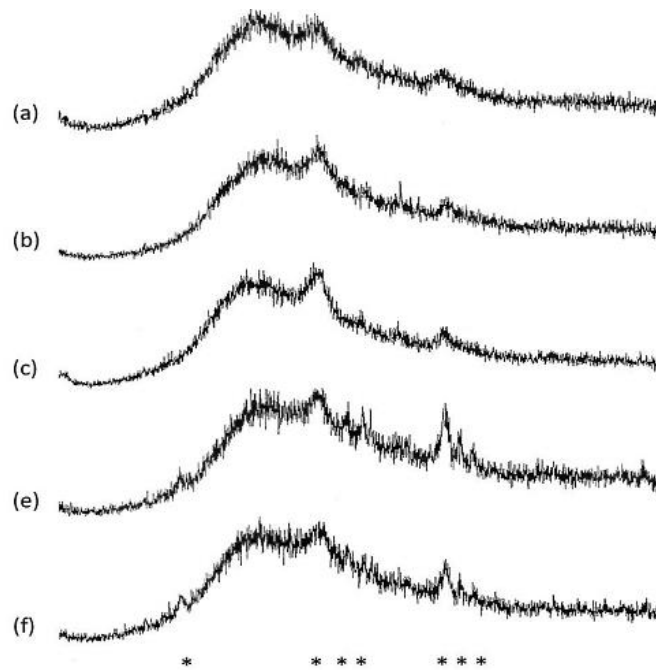


Fig. 4. XRD spectra for PES/FSHAp (a) 0.2, (b) 0.4, (c) 0.6, (d) 0.8 and (e) 1.0 IExM

3.2 Permeability Coefficient and Porosity of IExM

Pure water flux measurement was conducted to determine the permeability coefficient of the prepared membrane. Based on Figure 5 and Table 1, PES/HAp0.8 demonstrated the most promising properties with permeability coefficient and porosity of 101.5 L/m².h.bar and 87.69% respectively. By having the sharpest slope among other membranes, this kind of membrane was assumed to have the best permeability property. This finding was confirmed by the SEM image which showed a moderate amount of HAp successfully deposited onto PES membrane with low agglomeration rate.

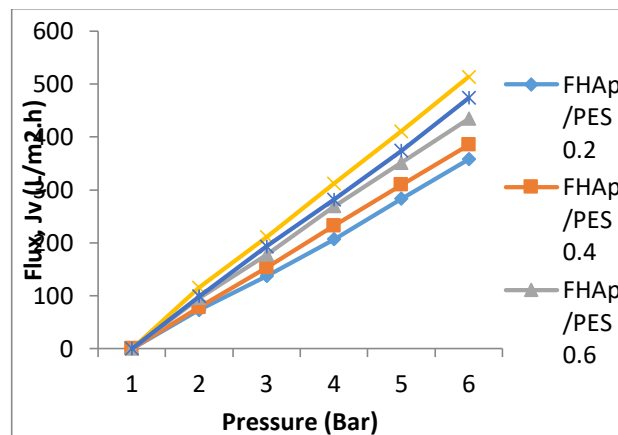


Fig. 5. Pure water flux of membranes modified with different FSHAp solution concentration

PES/HAp1.0 IExM has the highest and densest deposited HAp among all. Consequently, it will cause the membrane to be thicker. The porosity of membrane also greatly depended on the membrane thickness [22], as high amount of deposited HAp will also block the pores of a membrane which will increase the fouling rate. Therefore, PES/HAp-1.0 demonstrated poor performance when compared with PES/HAp0.8.

Table 1

Permeability coefficient, membrane thickness and porosity of hybrid membrane with different concentrations of FSHAP solution

Membrane ID	Permeability Coefficient (L/m ² .h.bar)	R ²	Membrane thickness (mm)	Porosity (%)
PES/HAp-0.2	71.09	0.999	0.078	67.78
PES/HAp-0.4	77.05	0.999	0.077	80.38
PES/HAp-0.6	86.61	0.999	0.075	87.2
PES/HAp-0.8	101.5	0.999	0.074	87.69
PES/HAp-1.0	93.75	0.999	0.074	87.36

3.5 Ion Exchange Capacity

IEC of IExM is directly proportional to the concentration of HAp solution used to modify the IExM. As the lower the concentration of HAp was used, there was less amount of HAp deposited onto the membrane surface, consequently, made the HAp tend to leak [23,24]. This can be explained with respect to decrease in fixed ion concentration with weak control of pathways for ion traffic (the crystallinity of the HAp itself also contribute major influence on the IEC performance) [25]. The uniform distribution, as well as the homogeneity of functional groups on the membrane surface, resulted in higher miscibility which can promote the more relative conducting regions and strengthen the intensity of the uniform electrical field around the membrane [27]. This result will lead to a decrease in the concentration polarization phenomenon [26]. A high amount of HAp will occupy the ionic pathways in the membrane matrix so that the space matrix will narrow and become limited [27]. Figure 6 showed PES/HAp 0.8 demonstrated optimum IEC with 49.44meq/g since it occupied the suitable amount of HAp which gives it better control on the pathways of ion traffic, thus, improves the membrane's IEC.

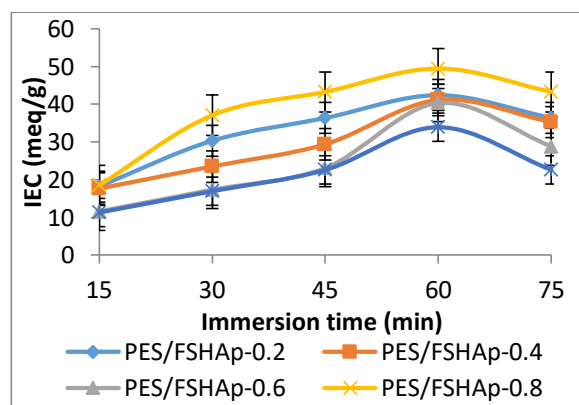


Fig. 6. IEC graph for each of the PES and PES/FSHApxxx IEM

3.6 Fouling Analysis

Due to the different charges, the protease molecule is likely to deposit onto the membrane surface and creating a cake layer which gives a major resistance for the fluids to pass through the membrane pores. According to result listed in Table 2, all these membranes demonstrated more than 50 % of flux recovery ratio with the highest relative flux reduction recorded was only 30.7%. This promising result was caused by the presence of HAp which has OH- groups that help to increase the hydrophilicity of the membrane, thus mitigating the membrane fouling [26,38].

Table 2
Fouling Analysis Data

Membrane ID	Flux Recover Ratio (%)	Relative Flux Reduction (%)
PES/HAp-0.2	69.3	30.7
PES/HAp-0.4	77.2	22.8
PES/HAp-0.6	77.7	22.3
PES/HAp-0.8	83.6	16.2
PES/HAp-1.0	82.3	17.7

The outstanding performance was demonstrated by the PES/HAp0.8 IExM with the highest FRR 83.6% and lowest RFF, 16.2% among others. Via SEM, AT-IR, and XRD, it showed that PES/HAp0.8 have a small size, well distributed and low agglomeration of HAp, high crystallinity and strong attachment onto PES membrane. These small size particles offer an extremely large surface area for water adsorption. Despite that, the less packed HAp when compared with HAp/PES 1.0 membrane deposited on the membrane surface also helps as it provides sufficient pores for solute transmission [28].

4. Conclusion

Among all fabricated IExMs, PES/HAp0.8 showed the best morphologies and characteristics. This was confirmed and evidenced via the results; XRD and FT-IR spectra. It indicates that the crystallinity of the HAp remained and there were peaks corresponding to the bonding of HAp and PES. These findings supported by the result obtained from performance tests applied in this research; pure water flux, porosity, swelling effect, IEC, ER, and fouling study. Thus, this study highly recommended using PES/HAp0.8 IExM for protease separation.

Acknowledgement

This research is fully supported by FRGS (vot 59354) grant. The authors fully acknowledged Ministry of Higher Education (MOHE) and Universiti Malaysia Terengganu for the approved fund which makes this important research viable and effective.

References

- [1] Santarelli, X., F. Domergue, G. Clofent-Sanchez, M. Dabadie, R. Grissely, and C. Cassagne. "Characterization and application of new macroporous membrane ion exchangers." *Journal of Chromatography B: Biomedical Sciences and Applications* 706, no. 1 (1998): 13-22.
- [2] Mah, Kor Zheng, and Raja Ghosh. "based composite lyotropic salt-responsive membranes for chromatographic separation of proteins." *Journal of Membrane Science* 360, no. 1-2 (2010): 149-154.

- [3] Suen, Shing-Yi, Yung-Chuan Liu, and Chao-Shuan Chang. "Exploiting immobilized metal affinity membranes for the isolation or purification of therapeutically relevant species." *Journal of Chromatography B* 797, no. 1-2 (2003): 305-319.
- [4] Kumbharkar, S. C., Y. Liu, and K. Li. "High performance polybenzimidazole based asymmetric hollow fibre membranes for H₂/CO₂ separation." *Journal of membrane science* 375, no. 1-2 (2011): 231-240.
- [5] García-Fernández, L., M. C. García-Payo, and M. Khayet. "Effects of mixed solvents on the structural morphology and membrane distillation performance of PVDF-HFP hollow fiber membranes." *Journal of membrane science* 468 (2014): 324-338.
- [6] Volkov, V. I., Yu M. Popkov, S. F. Timashev, D. G. Bessarabov, R. D. Sanderson, and Z. Twardowski. "Self-diffusion of water and fluorine ions in anion-exchange polymeric materials (membranes and resin) as determined by pulsed-field gradient nuclear magnetic resonance spectroscopy." *Journal of Membrane Science* 180, no. 1 (2000): 1-13.
- [7] Choi, Eun-Young, Heiner Strathmann, Ji-Min Park, and Seung-Hyeon Moon. "Characterization of non-uniformly charged ion-exchange membranes prepared by plasma-induced graft polymerization." *Journal of membrane science* 268, no. 2 (2006): 165-174.
- [8] Lalia, Boor Singh, Elena Guillen-Burrieza, Hassan A. Arafat, and Raed Hashaikeh. "Fabrication and characterization of polyvinylidene fluoride-co-hexafluoropropylene (PVDF-HFP) electrospun membranes for direct contact membrane distillation." *Journal of membrane science* 428 (2013): 104-115.
- [9] Scalera, F., F. Gervaso, K. P. Sanosh, A. Sannino, and A. Licciulli. "Influence of the calcination temperature on morphological and mechanical properties of highly porous hydroxyapatite scaffolds." *Ceramics International* 39, no. 5 (2013): 4839-4846. DOI: <https://doi.org/10.1016/j.ceramint.2012.11.076>
- [10] Barka, Nouredine, Samir Qourzal, Ali Assabbane, Abederrahman Nounah, and Yhya Ait-Ichou. "Removal of Reactive Yellow 84 from aqueous solutions by adsorption onto hydroxyapatite." *Journal of Saudi Chemical Society* 15, no. 3 (2011): 263-267.
- [11] Huang, Yi-Cheng, Pei-Chi Hsiao, and Huey-Jine Chai. "Hydroxyapatite extracted from fish scale: Effects on MG63 osteoblast-like cells." *Ceramics international* 37, no. 6 (2011): 1825-1831.
- [12] Sukaimi, J. A. M. A. L. I., S. O. F. I. A. H. Hamzah, and MOHD SABRI Mohd Ghazali. "Green Synthesis and Characterization of Hydroxyapatite From Fish Scale Biowaste." In *Applied Mechanics and Materials*, vol. 695, pp. 235-238. Trans Tech Publications, 2015.
- [13] Saravanabhavan, Shanmuga Sundar, and Sangeetha Dharmalingam. "Fabrication of polysulphone/hydroxyapatite nanofiber composite implant and evaluation of their in vitro bioactivity and biocompatibility towards the post-surgical therapy of gastric cancer." *Chemical engineering journal* 234 (2013): 380-388.
- [14] Hamzah, Sofiah, Jamali Sukaimi, and Mohd Sabri Mohd Ghazali. "Integration of Different Sintering Temperature of Hydroxyapatite and Polyethersulfone Membrane for Fouling Mitigation." In *Materials Science Forum*, vol. 863, pp. 154-159. Trans Tech Publications, 2016.
- [15] Klein, Elias. "Affinity membranes: a 10-year review." *Journal of Membrane Science* 179, no. 1-2 (2000): 1-27.
- [16] Hamzah, Sofiah, Nora'aini Ali, Abdul Wahab Mohammad, Marinah Mohd Ariffin, and Asmadi Ali. "Design of chitosan/PSf self-assembly membrane to mitigate fouling and enhance performance in trypsin separation." *Journal of Chemical Technology & Biotechnology* 87, no. 8 (2012): 1157-1166.
- [17] Nagahama, H., H. Maeda, T. Kashiki, R. Jayakumar, T. Furuike, and H. Tamura. "Preparation and characterization of novel chitosan/gelatin membranes using chitosan hydrogel." *Carbohydrate polymers* 76, no. 2 (2009): 255-260.
- [18] Luo, Ming-Liang, Jian-Qing Zhao, Wu Tang, and Chun-Sheng Pu. "Hydrophilic modification of poly (ether sulfone) ultrafiltration membrane surface by self-assembly of TiO₂ nanoparticles." *Applied Surface Science* 249, no. 1-4 (2005): 76-84.
- [19] Swain, Sanjaya Kumar, and Debasish Sarkar. "Study of BSA protein adsorption/release on hydroxyapatite nanoparticles." *Applied Surface Science* 286 (2013): 99-103.
- [20] Loghmani, Saeede Kuche, Morteza Farrokhi-Rad, and Taghi Shahrabi. "Effect of polyethylene glycol on the electrophoretic deposition of hydroxyapatite nanoparticles in isopropanol." *Ceramics International* 39, no. 6 (2013): 7043-7051.
- [21] Pang, Y. X., and Xujin Bao. "Influence of temperature, ripening time and calcination on the morphology and crystallinity of hydroxyapatite nanoparticles." *Journal of the European Ceramic Society* 23, no. 10 (2003): 1697-1704.
- [22] Ramesh, S., C. Y. Tan, W. H. Yeo, R. Tolouei, M. Amiriyan, I. Sopyan, and W. D. Teng. "Effects of bismuth oxide on the sinterability of hydroxyapatite." *Ceramics International* 37, no. 2 (2011): 599-606.
- [23] Khodabakhshi, A. R., S. S. Madaeni, T. W. Xu, L. Wu, C. Wu, C. Li, W. Na et al. "Preparation, optimization and characterization of novel ion exchange membranes by blending of chemically modified PVDF and SPPO." *Separation and purification technology* 90 (2012): 10-21.

- [24] Ma, Rui, Luqian Weng, Xujin Bao, Zhuo Ni, Shenhua Song, and Weiquan Cai. "Characterization of in situ synthesized hydroxyapatite/polyetheretherketone composite materials." *Materials Letters* 71 (2012): 117-119.
- [25] Klaysom, Chalida, Seung-Hyeon Moon, Bradley P. Ladewig, GQ Max Lu, and Lianzhou Wang. "Preparation of porous ion-exchange membranes (IEMs) and their characterizations." *Journal of membrane science* 371, no. 1-2 (2011): 37-44.
- [26] Hosseini, S. M., S. S. Madaeni, A. R. Heidari, and A. Amirimehr. "Preparation and characterization of ion-selective polyvinyl chloride based heterogeneous cation exchange membrane modified by magnetic iron–nickel oxide nanoparticles." *Desalination* 284 (2012): 191-199.
- [27] Sadat-Shojai, Mehdi, Mohammad-Taghi Khorasani, Ehsan Dinpanah-Khoshdargi, and Ahmad Jamshidi. "Synthesis methods for nanosized hydroxyapatite with diverse structures." *Acta biomaterialia* 9, no. 8 (2013): 7591-7621.
- [28] Jang, Suk Hyun, Young Gyu Jeong, Byung Gil Min, Won Seok Lyoo, and Sang Cheol Lee. "Preparation and lead ion removal property of hydroxyapatite/polyacrylamide composite hydrogels." *Journal of Hazardous Materials* 159, no. 2-3 (2008): 294-299.